#### **ORIGINAL INVESTIGATION**



### Radixin in the nucleus accumbens core modulates amphetamineinduced locomotor activity based on context association

Wen Ting Cai<sup>1</sup> · Myung Ji Kwak<sup>2</sup> · Joonyeup Han<sup>2</sup> · Haeun Rim<sup>2</sup> · Lars Björn Riecken<sup>3</sup> · Helen Morrison<sup>3</sup> · Wha Young Kim<sup>1</sup> · Jeong-Hoon Kim<sup>1,2</sup>

Received: 14 November 2024 / Accepted: 21 May 2025

© The Author(s), under exclusive licence to Springer-Verlag GmbH Germany, part of Springer Nature 2025

#### **Abstract**

Rationale The expression of addictive behaviors is linked to the structural plasticity of dendritic spines in the nucleus accumbens (NAcc). While radixin is known to contribute to morphological changes in dendritic spines, its role in the NAcc, specifically in the structural plasticity of dendritic spines and related drug-induced behavioral changes, is not well understood.

**Objective** In the present study, we investigated the effects of radixin manipulation in the NAcc core on amphetamine (AMPH)-induced locomotor activity, both in association with and independent of a specific environment. Additionally, we examined the accompanying changes in dendritic spine density in this region.

**Methods** We used a phosphomimetic pseudo-active mutant form (Rdx-T564D) and wild-type (Rdx-WT) radixin in conditioning and context-independent sensitization models induced by AMPH (1 mg/kg).

**Results** We observed that Rdx-T564D in the NAcc core selectively inhibited the expression of non-associative locomotor sensitization induced by AMPH. Conversely, overexpression of Rdx-WT in this region inhibited both conditioned locomotor activity and context-specific locomotor sensitization. Spine analysis revealed that the increase in mature thin spine density observed in the context-paired group was specifically suppressed by Rdx-WT, but not by GFP or Rdx-T564D.

**Conclusions** This study revealed that associative and non-associative forms of AMPH-induced reward memory are differentially regulated by radixin manipulation in the NAcc core, suggesting a critical role of radixin in psychomotor stimulant addiction.

Keywords Radixin · Nucleus accumbens · Dendritic spine · Amphetamine · Conditioning · Sensitization

- Wha Young Kim maru0222@yuhs.ac
- ☑ Jeong-Hoon Kim jkim1@yuhs.ac

Published online: 03 June 2025

- Department of Physiology, Yonsei University College of Medicine, 50-1 Yonsei-ro, Seodaemun-gu, Seoul 03722, Republic of Korea
- Department of Medical Sciences, Yonsei University College of Medicine, Seoul 03722, Republic of Korea
- <sup>3</sup> Leibniz Institute on Aging, Fritz Lipman Institute, 07745 Jena, Germany

#### Introduction

A hallmark of drug addiction is pathological craving, or an urge for drugs of abuse (Cheron and Kerchove d'Exaerde 2021; Tiffany and Wray 2012), which increases the risk of relapse in people with substance use disorders (SUD) (Jaffe et al. 1989; Preston et al. 1993). In rats, repeated exposure to psychostimulants, such as amphetamine (AMPH), leads to behavioral sensitization, manifested as an enhanced increase in locomotor activity when subsequently challenged with the drug following a withdrawal period. Behavioral sensitization is largely mediated by increased dopamine transmission in the mesolimbic dopamine system, and has been proposed as an animal model that reflects characteristics observed in people with SUD, such as escalation of drug use and long-lasting craving (Boileau et al. 2006; Robinson and Berridge 1993; Vezina 2004). Once



behavioral sensitization develops, it is maintained for a long period of time as a form of non-associative long-term memory and does not rely on specific contextual cues, distinguishing it from associative forms of learning, such as conditioning. However, individuals with SUD often experience strong cravings when exposed to drug-associated environments (Childress et al., 1986; Childs and de Wit 2013; O'Brien et al. 1992). In animal experiments, drugs of abuse often confer their locomotor activating and rewarding properties to the environments in which they were administered, resulting in the development of long-lasting conditioned effects from the environment, even in the absence of drugs (Anagnostaras et al. 2002; Stewart and Vezina 1988). Likewise in humans, with repeated drug use, a neutral stimulus in the environment where the drugs are taken can gradually acquire rewarding effects of drugs of abuse by forming a new associative memory between drugs and environment in the brain. This associative learning process binds specific sensory information to the rewarding effects of drugs, creating a memory link between drugs and the environment, which drives relapse and compulsive drug use in humans (Hyman et al. 2006).

Experience-dependent behavioral changes are associated with alterations in the quantity and structure of dendritic spines (i.e., structural plasticity) in relevant brain areas (Lamprecht and LeDoux 2004). For example, associative memory has been shown to increase the number of dendritic spines and change synaptic morphology in the hippocampus (Geinisman et al. 2001; Leuner et al. 2003). Structural plasticity of dendritic spines in the nucleus accumbens (NAcc), a central region in the brain's reward circuitry, is also implicated in drug abuse and contributes to the development of drug addiction (Nestler 2001; Robinson and Kolb 2004). The NAcc integrates dopaminergic inputs from the ventral tegmental area and glutamatergic inputs from the prefrontal cortex, hippocampus, and amygdala through extensive dendritic spines (Lanciego et al. 2012). This neuroanatomical connectivity positions the NAcc as an important neuronal substrate in the regulation of drug-related behaviors, including both conditioning and sensitization (Floresco 2015).

The dynamic reorganization of the actin cytoskeleton is crucial for dendritic spine plasticity (Schubert and Dotti 2007; Sekino et al. 2007). The ezrin, radixin, and moesin (ERM) proteins are key regulators in this process (Kawaguchi et al. 2017; Niggli and Rossy 2008). These proteins contribute to spine plasticity by linking the cytoskeleton to the plasma membrane when they become active through phosphorylation of their C-terminal threonine residue (Bosanquet et al. 2014). They also play a crucial role in regulating spine maturity. For instance, when ERM proteins are activated through phosphorylation, they bind to and assist cellular adhesion molecules in maintaining filopodia or spine

immaturity (Furutani et al. 2012; Raemaekers et al. 2012). Despite the crucial role of ERM proteins in regulating spine morphology, only a few studies have investigated their specific roles in the brain. For instance, ERM proteins have been shown to be involved in the formation of associative memory (Freymuth and Fitzsimons 2017; Hausrat et al. 2015). In addition, they have been also shown to be involved in the regulation of addictive behaviors. For example, AMPH and cocaine have shown to decrease the phosphorylation levels of ERM proteins in the NAcc core (Kim et al. 2009, 2013) and knocking down ezrin in this region has shown to reduce astroglial synaptic associations and increase cued heroin seeking (Kruyer et al. 2019). These results suggest that the activity of ERM proteins in the NAcc may play a significant role in the regulation of drugs of abuse.

We recently demonstrated that manipulating radixin activity via a phosphomimetic pseudo-active mutant form (Rdx-T564D) in the NAcc core disrupted sensitization to AMPH. In this process, we found that the expression of Rdx-T564D in the NAcc core prevents the increase in mature thin spines while augmenting filopodia-like thin spines, which are characterized by a small head and long length, suggesting that dynamic changes of thin spines in this region induced by the presence of Rdx-T564D might be an important regulator for the development of behavioral sensitization (Cai et al. 2022). However, these studies are limited by the addition of the mutant form of radixin that is in a constitutively active state and cannot be regulated through normal phosphorylation and dephosphorylation. Unlike Rdx-T564D, wild-type radixin (Rdx-WT) can cycle freely between phosphorylated and dephosphorylated states in response to local signaling cues (e.g., dopaminergic or glutamatergic input), which can result in alterations to spine morphology and behavioral output that significantly differ from those observed with Rdx-T564D. Furthermore, our previous studies measured only a non-associative form of behavioral changes. Therefore, in the present study, we aimed to expand our examination of radixin's role in regulating AMPH-induced behavioral changes both in association with and independent of a specific environment, using Rdx-WT as well as Rdx-T564D in the NAcc core.

#### **Materials and methods**

#### Subjects

Male Sprague-Dawley rats weighing 200–230 g (equivalent to 6 weeks olds) on arrival were obtained from Orient Bio Inc. (Seongnam-si, Korea). They were housed as three per cage in a 12-h light/dark cycle room (lights out at 8:00 pm) and all experiments were conducted during the day time.



Rats had access to food and water *ad libitum* at all times. All experiments were started a week after arrival to allow habituation to a new colony environment. All animal use procedures were conducted according to an approved Institutional Animal Care and Use Committee protocol of Yonsei University College of Medicine (protocol number 2017 –0194).

#### Virus

The plasmids for lentiviral vectors containing copepod green fluorescent protein (copGFP) alone, or copGFP with Rdx wild-type (Rdx-WT) or Rdx T564D, were designed and kindly provided by Drs. Lars Björn Riecken and Helen Morrison at the Leibniz Institute on Aging, Fritz Lipmann Institute (Jena, Germany). In brief, human radixin gene either wild-type or with a mutation at the threonine 564 amino acid residue, changing it to aspartic acid, and an additional FLAG-tag sequence (GACTACAAGGACGACGA C) at the N-terminal, were cloned in the lentiviral pCDH-CuO-MCS-EF1-copGFP vector (SparQ Dual Promoter, System Biosciences) (Riecken et al. 2016). Virus particles were generated using a third-generation lentiviral packaging systems at the Virus Facility, Research Animal Source Center, Korea Institute of Science and Technology (Seoul, Korea).

#### **Surgery for virus infusion**

Rats were anesthetized with intraperitoneal (IP) ketamine (100 mg/kg) and xylazine (6 mg/kg), placed in a stereotaxic instrument with the incisor bar at 5.0 mm above the interaural line. Infusion cannulas (28 gauge, Plastics One, Roanoke, VA, USA) connected to 2 µl Hamilton syringes (Reno, NV, USA) via PE-20 tubing were angled at 10° to the vertical and bilaterally lowered into the NAcc core (A/P,  $\pm 3.2$ ; L,  $\pm 2.8$ ; D/V, -7.1 mm from bregma and skull). 1  $\mu$ l (1 × 10<sup>12</sup> particles/ml) of lentiviral constructs, containing copGFP alone, or copGFP with Rdx-WT or Rdx-T564D, were then bilaterally infused for 5 min and another 5 min allowed for diffusion before the infusion cannulas were taken out. After viral infection was finished, the incised skin covering the skull was grabbed with surgical staplers. Then, rats were returned to their home cages for recovery.

#### Drugs

D-amphetamine sulfate (United States Pharmacopeial, Rockville, MD, USA) was dissolved in sterile 0.9% saline to a final working concentration of 1 mg/ml.

#### **Experimental design and procedures**

Upon arrival, all rats underwent a week-long adaptation period in their new housing environment, and three separate experiments were conducted.

**Experiment 1 (spine analysis)** Rats were arbitrarily divided into three groups, without specific randomization methods. Each group was surgically injected with viruses containing GFP, Rdx-WT, or Rdx-T564D respectively. After two weeks in the home cage, the rats were transcardially perfused, and their brains were removed. Dendritic spine analysis was conducted using immunohistochemistry and confocal imaging. A total of 9 rats (GFP 3, Rdx-WT 4, Rdx-T564D 2) were used and all included in the statistical analysis.

Experiment 2 (context-independent AMPH sensitization) Rats were arbitrarily divided into three groups, following the same method described in Experiment 1. They were surgically injected with viruses containing GFP, Rdx-WT, or Rdx-T564D respectively. Once the rats recovered from surgery, each group was further arbitrarily divided into two subgroups and pre-exposed to either saline or AMPH (1.0 mg/ kg, IP) with a total of four injections, given 2.3 days apart. This regimen of drug injection is known to produce enduring sensitization of the locomotor response to AMPH (Jang et al. 2018; Kim et al. 2001). To avoid confounding effects of conditioning, AMPH was administered in different environments (i.e., in the activity boxes for the first and fourth injections, and in their home cages for the other injections). Two weeks after the last pre-exposure injection, all rats were habituated to the activity boxes for 30 min, after which they were injected with AMPH (1.0 mg/kg, IP), and their locomotor activity was measured for 1 h. The next day, the rats were transcardially perfused, and their brains were removed for histological verification of viral expression. Viral expression was targeted to the NAcc core for rats included in the analysis (Fig. S1). A total of 57 rats (GFP 19, Rdx-WT 25, Rdx-T564D 13) were used and all included in the statistical analysis.

Experiment 3 (conditioned locomotion and context-specific AMPH sensitization) Rats were arbitrarily divided into three groups, following the same procedure described in Experiment 1. They were surgically injected with viruses containing GFP, Rdx-WT, or Rdx-T564D respectively. After 2 weeks of surgical recovery, rats with different viruses were randomly assigned to two groups according to the conditioning paradigm. During the development of conditioning, rats received IP injections of saline or AMPH in five 2-day blocks. For each block, rats were administered saline in their home cages on day 1 and AMPH (1 mg/kg, IP) in the



locomotor activity boxes on day 2 (paired), or saline in both environments (control). For the conditioning test, 1 week after the last conditioning block, all rats were tested for their conditioned locomotor response in the activity boxes for 1 h following an IP saline injection. Additionally, a sensitization test was conducted 3 days after the conditioning test. On the test day, all rats were habituated to the locomotor activity boxes for 30 min and then tested for their locomotor response in the activity boxes for 1 h following an AMPH (1 mg/kg, IP) challenge. The next day, the rats were transcardially perfused, and their brains were removed for histology verification and spine analysis. Viral expression was targeted to the NAcc core for rats included in the analysis (Fig. S2). A total of 39 rats (GFP 16, Rdx-WT 11, Rdx-T564D 12) were used and all included in the statistical analysis.

Experiment 4 (western blotting of total and phosphorylated ERM by GFP, Rdx-WT, Rdx-T564D) Rats were arbitrarily divided into three groups, in the same way as described in the Experiment 1, and they were surgically injected with viruses containing GFP, Rdx-WT or Rdx-T564D, respectively. After two weeks at home cage, rats were administered a single IP injection of either Saline or AMPH (1 mg/ kg). Then, after 60 min, they were decapitated, and their brain tissues, specifically the NAcc core containing GFP, were dissected and collected by an experimenter wearing barrier filter glasses, using a flashlight (Nightsea, Bedford, MA, USA) with a blue LED to excite green fluorescence. The tissues were then prepared for western blot analysis. Viral expression was targeted to the NAcc core for rats included in the analysis. A total of 37 rats (GFP 12, Rdx-WT 12, Rdx-T564D 13) were used and all included in the statistical analysis.

**Experiment 5 (GFP and GluA1 immunohistochemistry)** Rats were first surgically injected with viruses containing GFP. After two weeks at home cage, they were perfused, and their brain tissues (the NAcc core) were prepared for immunohistochemistry. A total of 2 rats were used for analysis.

#### **Locomotor activity**

Locomotor activity was measured with a bank of 9 activity boxes (35 × 25 × 40 cm) (IWOO Scientific Corporation, Seoul, Korea) made of translucent Plexiglas. Each box was individually housed in a PVC plastic sound attenuating cubicle. The floor of each box consisted of 21 stainless steel rods (5 mm diameter) spaced 1.2 cm apart center-to-center. Two infrared light photobeams (Med Associates, St. Albans, VT, USA), positioned 4.5 cm above the floor and spaced evenly along the longitudinal axis of the box, were used to estimate locomotor activity.



Rats were all deeply anesthetized with ketamine (100 mg/kg) and xylazine (6 mg/kg) and then perfused transcardially with 10 mM phosphate buffered saline (PBS) (pH 7.4) followed by 4% paraformaldehyde (PFA) solution in 10 mM PBS (pH 7.4). The brains were removed and transferred to 4% PFA in 10 mM PBS (pH 7.4) for another 24 h. Then, brains were washed with 10 mM PBS, cryoprotected in 30% sucrose solution and stored at -80 °C.

Free-floating 100 µm sections from frozen tissue blocks were prepared on a cryostat (HM 525; Thermo Scientific, Waltham, MA, USA). For enhanced visualization of GFP signals in infected neurons, GFP immunostaining was performed. The tissue sections were blocked for 1 h in 10 mM PBS containing 5% normal goat serum (Jackson ImmunoResearch Laboratories, West Grove, PA, USA) and 0.3% triton X-100. Then, they were incubated overnight with the anti-TurboGFP antibody (1:1,000; Evrogen, Moscow, Russia), diluted in 10 mM PBS containing 2% normal goat serum and 0.1% triton X-100 at 4 °C. Next day, the sections were rinsed 3 times in 10 mM PBS containing 0.1% triton X-100 and incubated with the anti-rabbit IgG antibody coupled to Alexa 488 (1:2,000; Invitrogen, Waltham, MA, USA) for 2 h at 24 °C. They were rinsed again and cover-slipped with Vectashield mounting medium (Vector Laboratories, Burlingame, CA, USA).

#### Spine imaging and analysis

For spine analysis, individual dendritic segments of medium spiny neurons (MSNs) were imaged based on published requirements (Cahill et al. 2018): (1) the segments have to appear uniform GFP distribution, (2) the segments cannot be overlapped with other neighboring dendritic segments and be traced back to their soma, (3) secondary and tertiary dendritic segments are chosen at least 50 µm away from soma. We imaged 1 to 3 dendrites per neuron and two to seven neurons per rat. Spine analyses were conducted by experimenter who knew only tissue numbers, but was blind to what group they belong. The spine counting results were first analyzed based on the number of neurons and then based on the number of animals (see Supplementary Information).

All images were acquired under a LSM700 confocal laser scanning microscope (Carl Zeiss, Oberkochen, Germany) with a 488 nm argon laser. For whole cell reconstructions, confocal stacks of MSNs were imaged at 20x air objective lens (numerical aperture 0.7) with a Z-step size of 0.99 µm and an XY resolution of 0.417 µm. For dendrite imaging, dendritic segments stacks spaced 0.2 µm were acquired with a 63x oil-immersion objective (numerical aperture 1.4) and



a scan zoom of 3.0. The pinhole aperture set to 1 Airy Unit and the line average of 2 was used. The full dynamic ranges of images were obtained by adjusting the laser intensity and photomultiplier tube gain. All images were taken with a resolution of 1024 pixels in X dimension and the Y dimension within the frame was cropped to  $\sim\!300$  pixels according to particular dendritic segments for fast image acquisition and the pixel dwell time was 1.58  $\mu$ m/s. The final voxel size was 0.033  $\times$  0.033  $\times$  0.2  $\mu$ m<sup>3</sup> in X-Y-Z plane.

To improve contrast and resolution, raw confocal images were deconvolved with AutoQuant X3 deconvolution software (Media Cybernetics, Inc, Rockville, MD, USA). Dendrite tracing and automatic spine detection was then performed using NeuronStudio software (courtesy of Icahn School of Medicine at Mount Sinai, New York, USA) with Rayburst algorithm, which classifies spines into thin, mushroom or stubby according to the classification dimensions (i.e. neck ratio, thin ratio, mushroom size) (Rodriguez et al. 2008). The minimum and maximum spine height values were set at 0.5  $\mu m$  and 3.0  $\mu m$ , respectively. 22 voxels were set for minimum stubby size based on published criteria (Jung et al. 2013).

### Tissue preparation and immunohistochemistry for GFP and GluA1

Rats were deeply anesthetized with intraperitoneal (IP) ketamine (100 mg/kg) and xylazine (6 mg/kg) and perfused with intracardially with 10 mM phosphate buffered saline (PBS, pH 7.4). Thereafter, the brains were quickly removed and immediately cut into blocks containing NAcc on an ice cold dish. The tissue blocks were then plunged into 4% paraformaldehyde (in 10 mM PBS, pH 7.4) and maintained for one hour. After rinsed with 10 mM PBS, tissue blocks were transferred to 30% sucrose and stored overnight at 4 °C. Tissue blocks were embedded and stored at -80 °C on the next day.

For immunofluorescence staining, free-floating brain Sect. (100 µm) from frozen tissues were prepared on a freezing microtome (HM 525, Thermo Scientific, Waltham, MA, USA). They were blocked for 1 h in 10 mM PBS containing 5% normal goat serum (Vector laboratories, Burlingame, CA, USA) and 0.3% triton X-100 and then incubated overnight with mixture of anti-GFP (1:1000, Abcam, Cambridge, UK) with anti-GluA1 antibodies (1:1000, Millipore, USA), diluted in 10 mM PBS containing 2% normal goat serum and 0.1% triton X-100 at 4 °C. Following overnight incubation, sections were rinsed 3 times for 10 min in 10 mM PBS containing 0.1% triton X-100 and incubated for 2 h with the secondary antibodies which were goat anti-chicken Alexa Fluor 488 (1:1000, Thermo Scientific, Waltham, MA, USA) and goat anti-rabbit Alexa Fluor 568

(1:1000, Thermo Scientific, Waltham, MA, USA) at room temperature in the same diluent as primary antibodies. After 2 h, they were rinsed 3 times for 10 min again in 10 mM PBS containing 0.1% triton X-100 and cover-slipped with Vectashield mounting medium H1400 (Vector laboratories, Peterborough, UK).

For visualizing GFP and GluA1 immunoreactivity, immunofluorescence sections were examined under LSM700 confocal laser scanning microscope (Carl Zeiss, Oberkochen, Germany) equipped with diode lasers at wavelength of 488 and 555 nm. For high-magnification 3D images, each NAcc region of image stacks spaced by 0.2  $\mu$ m in z plane were acquired as  $1024 \times 1024$  pixels per x-y frame with 1 Airy unit of optical thickness with 63x oil immersion objective (Numerical aperture 1.4) and a scan zoom of 3.0. Scan averaging was set to 4 to improve signal to noise ratio of each optical section. After acquisition, images were deconvoluted using Imaris software (Bitplane) for improving contrast and resolution. The colocalization analysis was performed using ZEN image analysis software (Carl Zeiss).

#### **Western blotting**

Tissues were homogenized in lysis buffer (pH 7.4) containing 0.32 M sucrose, 2 mM EDTA, 1% SDS, 10 µg/ ml aprotinin, 10 µg/ml leupeptin, 1 mM phenylmethylsulfonyl fluoride, 10 mM sodium fluoride, and 1 mM sodium orthovanadate. The concentration of protein was determined by using Pierce BCA Protein Assay Kit (Cat. No. 23227, Thermo Scientific Inc., Rockford, IL, USA). Samples were then boiled for 10 min and subjected to SDS-polyacrylamide gel electrophoresis. Proteins were separated and transferred electrophoretically to nitrocellulose membranes (Cat. No. 1620094, Bio-Rad, Hercules, CA, USA), which were then blocked with 5% bovine serum albumin (BSA) in PBS-T buffer [10 mM phosphate-buffered saline plus 0.05% Tween-20]. Specific antibodies against phospho-ERM (1:500, specific to detect phosphorylated ezrin-radixinmoesin at threonine 567, 564 or 558, respectively; Abcam, Cambridge, UK), ERM (1:500, Cell Signaling, Beverly, MA, USA) or α-tubulin (1:50000; Santa Cruz, Dallas, TX, USA) were diluted in PBS-T with 5% bovine serum albumin, and used to probe the blots. Primary antibodies were detected with peroxidase-conjugated secondary antibodies against rabbit IgG (1:2,000; KOMA Biotech, Seoul, Korea) or mouse IgG (1:5000; Cell Signaling, Beverly, MA, USA) diluted in PBS-T with 5% skim milk, followed by enhanced chemiluminescence reagents (Amersham Biosciences, Arlington Heights, IL, USA) and exposure to X-ray film. Band intensities were quantified based on densitometric values using Fujifilm Science Lab 97 Image Gauge software (version 2.54) (Fujifilm, Tokyo, Japan).



#### Statistical analyses

Statistical analyses were performed using GraphPad Prism (version 8.0.1). The data were analyzed with one-way or two-way analysis of variance (ANOVA), followed by Bonferroni *post hoc* test. Differences between experimental conditions were considered statistically significant when p < 0.05.

#### **Results**

### Rdx-WT and Rdx-T564D increase filopodia-like thin spines in the NAcc core

We first examined the effects of Rdx-WT and Rdx-T564D in the NAcc core on the morphological changes of dendritic spines. The surgical target area, where the viruses were microinjected, along with representative images showing the MSNs and a dendritic segment indicating different subtypes of spines, are shown in Fig. 1A. The densities of the total spines and each spine subtype were counted from dendritic segments of several randomly selected MSNs (7 to 12 neurons per group) expressing different virus types in the NAcc core (Fig. 1B). One-way ANOVA conducted on the total spine density revealed a significant effect between groups  $(F_{2,24} = 5.282, p < 0.05)$ . Post hoc Bonferroni comparisons showed that total spine density was significantly increased (p < 0.05) in rats with Rdx-WT or Rdx-T564D compared to rats with GFP (Fig. 1B). Among the spine subtypes, thin spines were further categorized into two types: filopodia-like (immature), with head diameter less than 0.2 µm and spine length greater than 1.5 µm, and mature thin spines for the rest following our previous criteria (Cai et al. 2022). The densities of the thin spines (filopodia-like), but not other subtypes, were also found to be increased in rats with Rdx-WT or Rdx-T564D compared to rats with GFP (Fig. 1B, Fig. S3).

Next, to examine whether thin spines with small head and long length that we characterized as immature exhibit AMPA receptor subunits, we observed co-labelling of GFP with GluA1, specific maker for mature spines (Vardalaki et al. 2022), after two weeks of virus injection. High magnification confocal microscopy images revealed that GluA1 was co-localized with mature spines (mushroom spines or mature thin spines, whereas GluA1 was absent from filopodia-like (immature) thin spines (Fig. S4).

## Context-independent sensitization was selectively inhibited by Rdx-T564D, but not by Rdx-WT, in the NAcc core

As we previously demonstrated that Rdx-T564D in the NAcc core inhibits the context-independent form of

Fig. 1 Effects of Rdx-WT and Rdx-T564D expression on spine densities in the NAcc core. A The NAcc core region where viruses were injected is schematically illustrated (dark grey area). A representative low magnification (2x) epifluorescence image (scale bar: 500 μm) of the NAcc core, and a higher magnification (20x) confocal microscopy image (scale bar: 50 µm) of a single neuron in this region, expressing lentivirus-mediated copepod green fluorescent protein (copGFP) are shown. A 3D reconstruction image (scale bar: 5 µm) of a GFP-labelled dendritic segment showing spine subtypes is also shown. B Representative high resolution images of a dendritic segment labelled with GFP from each group. Scale bar is 5 µm. Significant differences of densities were observed for total and filopodia-like thin spines. \*p< 0.05, \*\*p< 0.01 compared to GFP control group. Data are shown as mean + standard error of mean (SEM). Numbers of neurons analyzed for each group are as follows: GFP (8 neurons from 3 rats), Rdx-WT (12, 4), Rdx-T564D (7, 2)

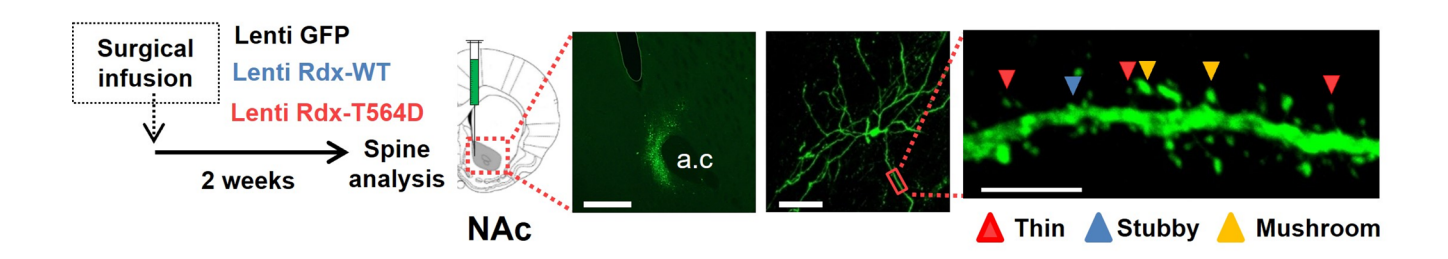
locomotor sensitization by AMPH (Cai et al. 2022), we aimed to further investigate whether Rdx-WT would have the same effect. The experimental scheme, from virus injection surgery to locomotor sensitization, is illustrated in Fig. 2A. Rats were pre-exposed to either saline or AMPH (1.0 mg/kg, IP) with a total of four injections administered 2-3 days apart. AMPH was administered in different environments (activity box and home cage) to avoid any confounding effects of conditioning. Two-way ANOVA conducted on the 1-h total locomotor activity counts revealed a significant effect of pre-exposure  $(F_{1.51} =$ 9.814, p < 0.01). Post hoc Bonferroni comparisons showed that locomotor activity was significantly increased (p< 0.05) in AMPH pre-exposed rats compared to saline preexposed rats with GFP or Rdx-WT viruses, whereas these effects were absent in AMPH pre-exposed rats with Rdx-T564D virus (Fig. 2B). Additionally, post hoc Bonferroni comparisons within the AMPH pre-exposure group showed a significant decrease in locomotor activity in Rdx-T564D compared to GFP (p < 0.05) (Fig. 2B).

## Conditioned locomotion and context-specific sensitization were selectively inhibited by Rdx-WT, but not by Rdx-T564D, in the NAcc core

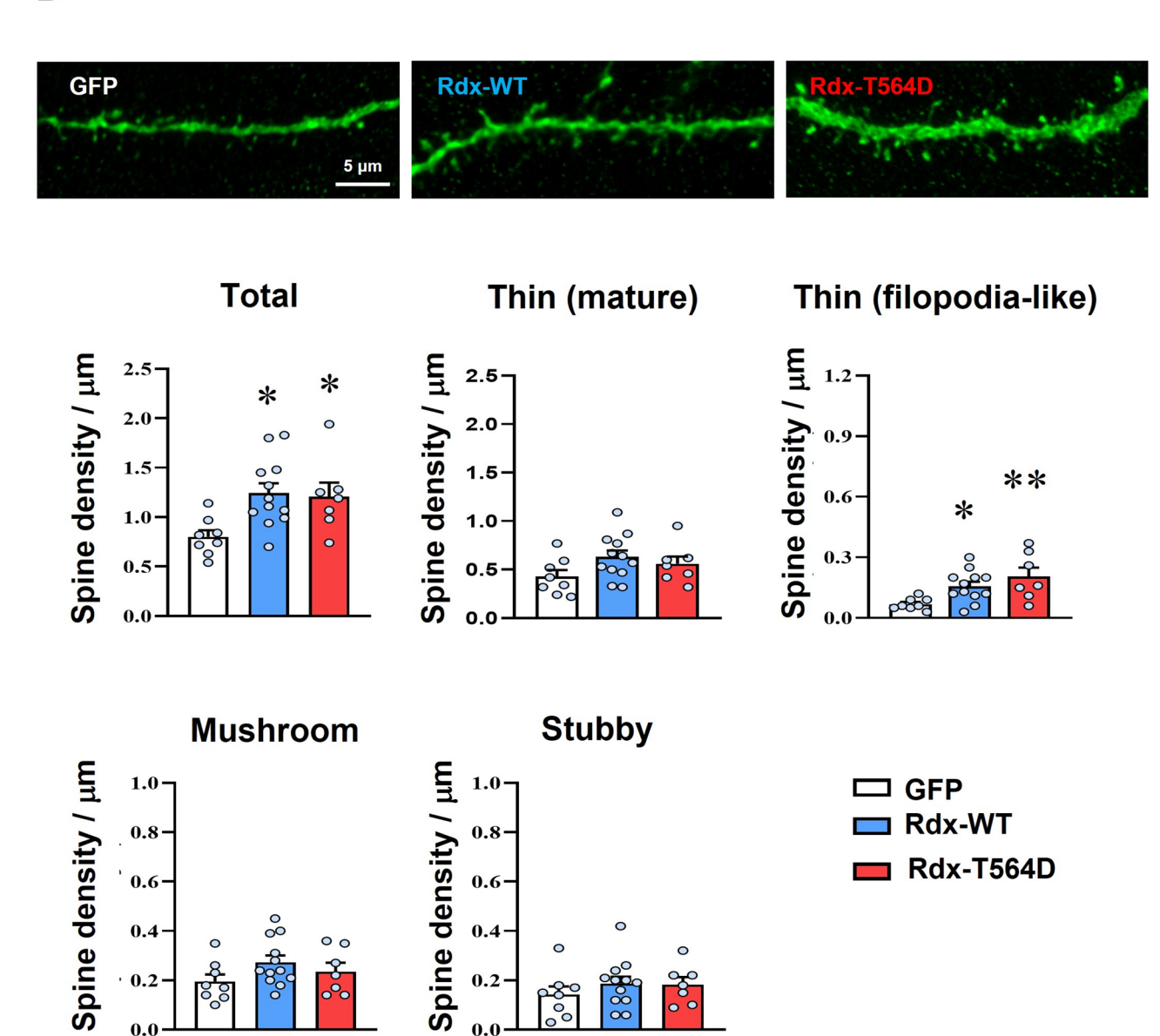
To further explore the functional effects of radixin on the expression of AMPH-induced locomotor activity, we examined its effects on conditioned locomotion and context-specific sensitization. The experimental scheme, from virus injection surgery to the development of conditioning and challenge tests, is illustrated in Fig. 3A. Rats in the paired group were repeatedly administered AMPH (1.0 mg/kg, IP) in the locomotor activity box and saline in the home cage, while those in the control group received saline in both places. One week after the last pairing, the rats were tested with saline for conditioned locomotion. Two-way ANOVA conducted on the 1-h total locomotor activity counts revealed significant effects of conditioning groups



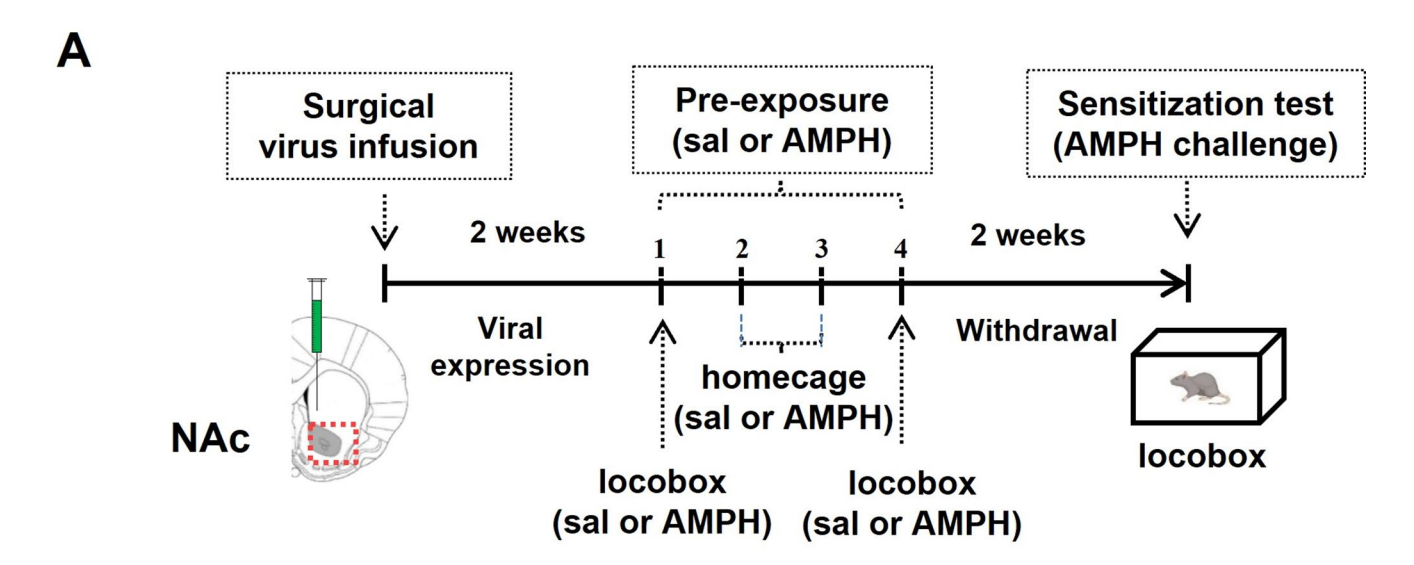




В







### B Context-independent sensitization

**AMPH** 

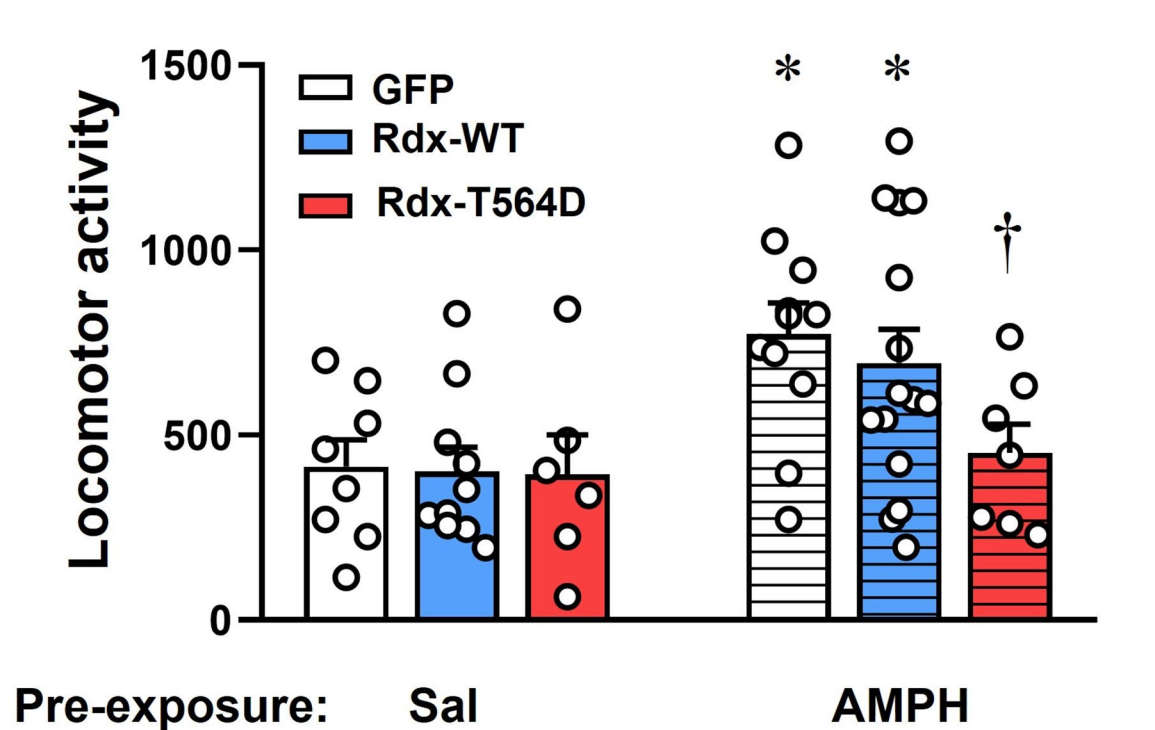


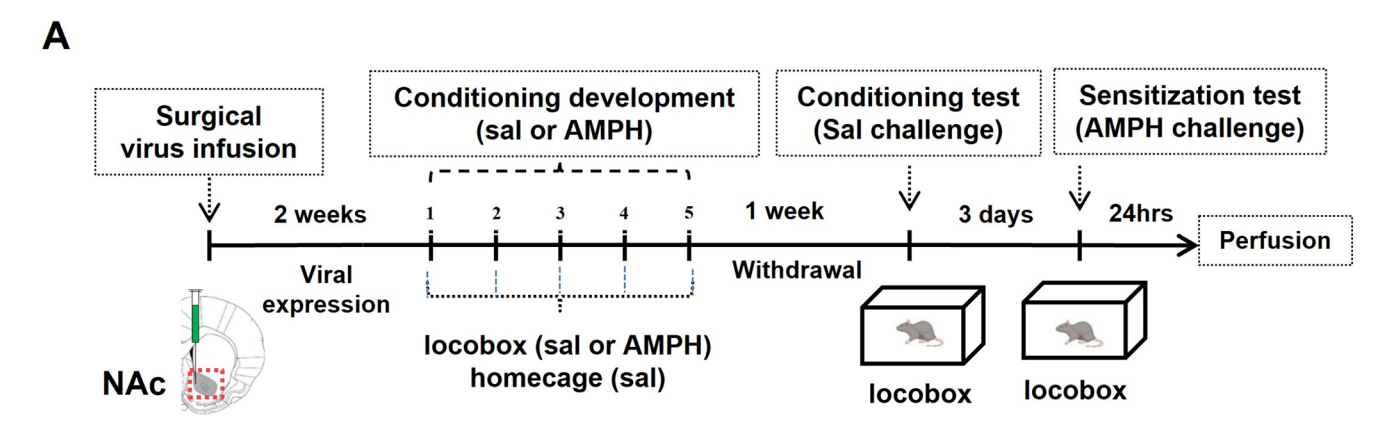
Fig. 2 Context-independent sensitization was selectively inhibited by Rdx-T564D, but not by Rdx-WT, in the NAcc core. A Timelines for the experimental procedures indicate the duration of virus expression and the locomotor sensitization scheme. B Total locomotor activity counts observed during the 60 min test on AMPH challenge are shown as group mean + SEM. \* p<0.05, compared between saline and

Challenge:

AMPH pre-exposure within GFP or Rdx-WT. † p< 0.05, compared between GFP and Rdx-T564D within AMPH pre-exposure. Numbers of rats analyzed for each group are as follows: In saline pre-exposures, GFP (8), Rdx-WT (10), and Rdx-T564D (6); In AMPH pre-exposures, GFP (11), Rdx-WT (15), and Rdx-T564D (7)

**AMPH** 





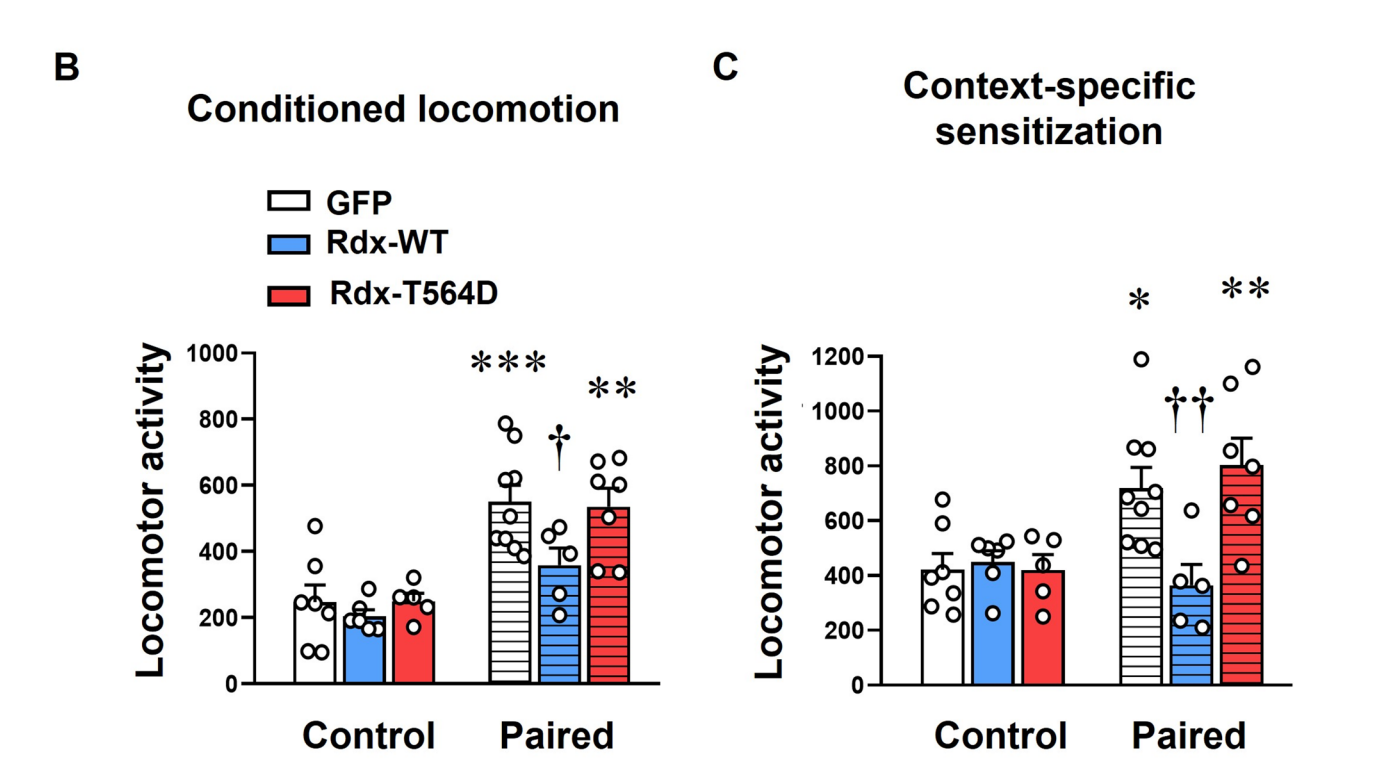


Fig. 3 Conditioned locomotion and context-specific sensitization were selectively inhibited by Rdx-WT, but not by Rdx-T564D, in the NAcc core. A Timelines for the experimental procedures indicate the duration of virus expression and behavioral scheme (conditioning and sensitization). B Total locomotor activity counts observed during the 60 min test on saline challenge are shown as group mean +SEM. \*\*\* p < 0.001, \*\* p < 0.01, compared to GFP or Rdx-T564D within control group. † p < 0.05, compared to GFP within the paired group. C Total

locomotor activity counts observed during the 60 min test on AMPH challenge are shown as group mean +SEM. \* p< 0.05, \*\* p< 0.01, compared to GFP or Rdx-T564D within control group. †† p< 0.01, compared to GFP or Rdx-T564D within the paired group. Numbers of rats analyzed for each group are as follows: In control groups, GFP (7), Rdx-WT (6), and Rdx-T564D (5); In paired groups, GFP (9), Rdx-WT (5), and Rdx-T564D (7)

( $F_{1, 33} = 38.4, p < 0.001$ ) and virus type ( $F_{2, 33} = 3.427, p < 0.05$ ). As expected, rats with GFP in the paired group exhibited increased conditioned locomotion compared to the control group (p < 0.001; post hoc Bonferroni comparisons). Interestingly, these effects were persisted in the paired group with Rdx-T564D (p = 0.001), whereas they were absent in the paired group with Rdx-WT (Fig. 3B). Post hoc

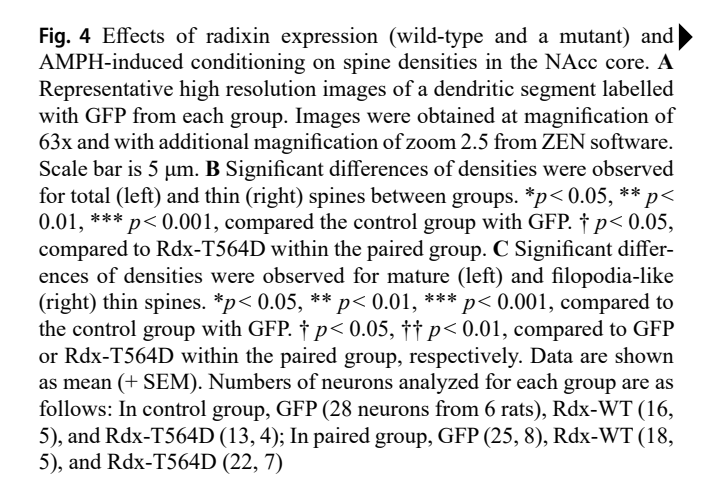
Bonferroni comparisons within paired groups revealed that the increase in conditioned locomotion was significantly inhibited (p< 0.05) in rats with Rdx-WT compared to rats with GFP (Fig. 3B). Time-course analysis of these findings showed that Rdx-WT's ability to inhibit conditioned locomotion in the AMPH-paired group was evident throughout the 1-h time course (Fig. S5 A).



Three days after measuring conditioned locomotion, rats were tested with an AMPH challenge for context-specific sensitization. Two-way ANOVA conducted on the 1-h total locomotor activity counts showed significant effects of conditioning groups ( $F_{1,33} = 10.23$ , p < 0.01), virus types  $(F_{2,33} = 3.709, p < 0.05)$ , and conditioning group x virus type interactions ( $F_{2,33} = 4.92$ , p < 0.05). As with conditioned locomotion, rats with GFP in the paired group exhibited context-specific locomotor sensitization compared to the control group (p < 0.05; post hoc Bonferroni comparisons). Similarly, these effects were also present in the paired group with Rdx-T564D (p < 0.01), whereas they were absent in the paired group with Rdx-WT (Fig. 3C). Post hoc Bonferroni comparisons between paired groups revealed that the increase in context-specific locomotor sensitization was significantly inhibited (p < 0.01) in rats with Rdx-WT (Fig. 3C). Time-course analysis of these findings showed that Rdx-WT's ability to inhibit context-specific locomotor sensitization in the AMPH-paired group was evident throughout the 1-h time course (Fig. S5B).

## Rdx-WT and Rdx-T564D in the NAcc core differentially regulate the density of mature thin spines in the expression of conditioned behaviors

After the completion of the conditioned behavioral challenge test, the rats' brains were removed and dendritic spines were analyzed. Representative dendritic segments from different groups are shown in Fig. 4A. Two-way ANOVA conducted on total spine density revealed a significant effect of conditioning group x virus type interactions  $(F_{2.116} = 4.057, p < 0.05)$ . Post hoc Bonferroni comparisons showed that total spine density was significantly increased in the paired group, compared to the control group, with GFP (p < 0.05). Notably, post hoc Bonferroni comparisons within paired groups revealed that these effects seen with GFP were significantly reduced with Rdx-WT group compared to the Rdx-T564D group (p < 0.05), whereas they were maintained with Rdx-T564D (p < 0.01) (Fig. 4B, left). Further analysis of spine subtypes revealed that the increase in total spine density was largely owing to an increase in thin spines, with no significant changes observed in mushroom or stubby spines (Fig. 4B, right; Fig. S6). Two-way ANOVA conducted on thin spine density showed significant effects of virus type ( $F_{2,116} = 3.868$ , p < 0.05) and conditioning group x virus type interactions ( $F_{2.116} = 4.802$ , p <0.05). Post hoc Bonferroni comparisons revealed that thin spine densities were significantly increased in the paired group, compared to the control group, with GFP (p < 0.05) and Rdx-T564D (p < 0.001). However, these effects were not observed in the paired group with Rdx-WT, and post hoc Bonferroni comparisons between paired groups showed



that the effects seen with GFP were significantly reduced with Rdx-WT group compared to the Rdx-T564D group (p < 0.01) (Fig. 4B, right).

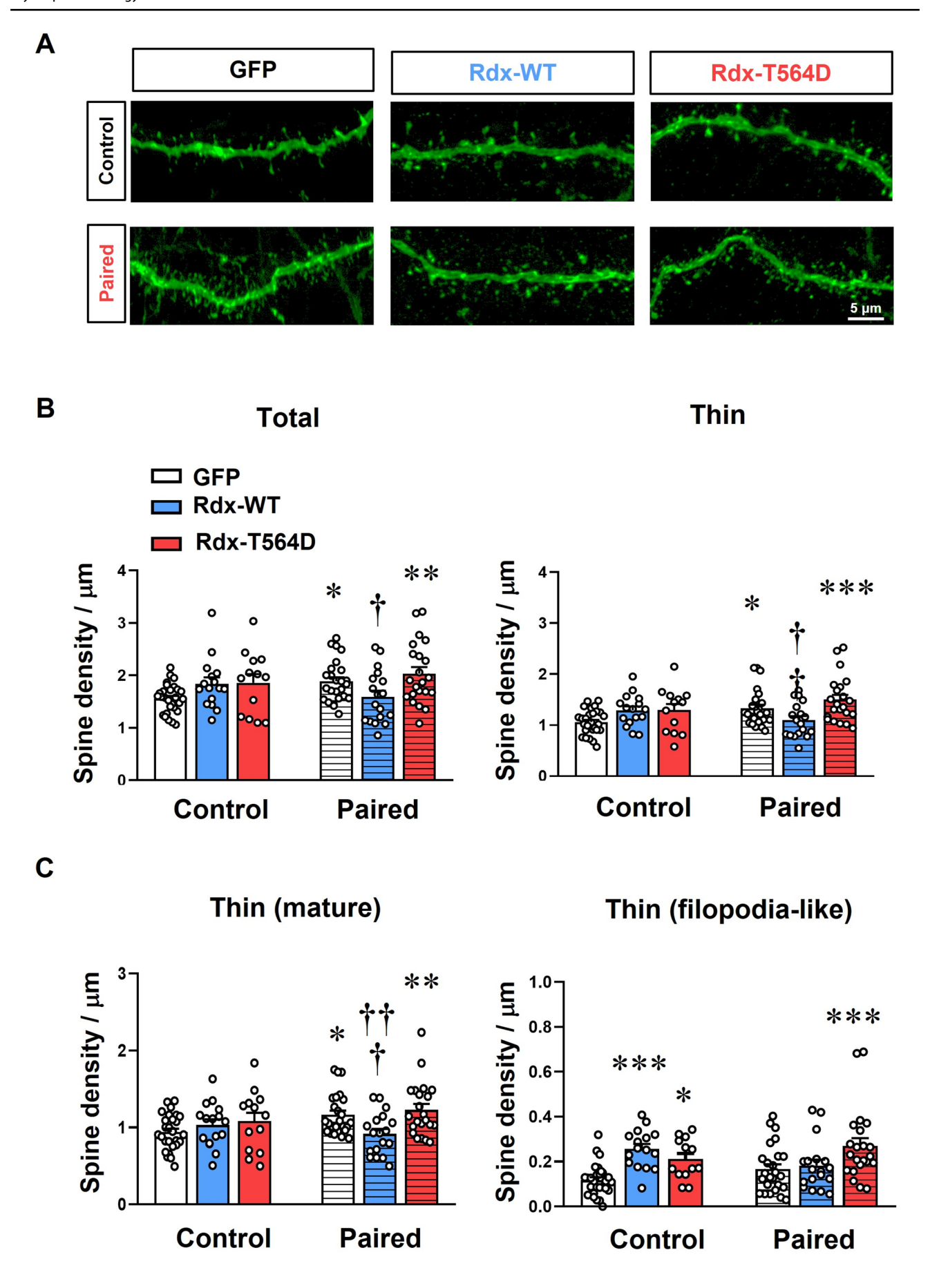
To further delineate these changes, thin spines were categorized into filopodia-like (immature) and mature subtypes as described above for Fig. 1, and their densities were reanalyzed. A two-way ANOVA performed on the mature thin spine density revealed significant effects of virus type ( $F_{2, 116} = 3.138, p < 0.05$ ) and conditioning group x virus type interactions ( $F_{2, 116} = 3.562, p < 0.05$ ). Post hoc Bonferroni comparisons showed that mature thin spine density was significantly increased in the paired group, compared to the control group, with GFP (p < 0.05). Notably, post hoc Bonferroni comparisons within the paired groups showed that the effects observed with GFP were significantly reduced with Rdx-WT (p < 0.01), whereas they were maintained with Rdx-T564D (p < 0.01) (Fig. 4C, left).

Meanwhile, a two-way ANOVA performed on filopodialike thin spine density revealed significant effects of virus type ( $F_{2, 116} = 10.1, p < 0.001$ ) and conditioning group x virus type interactions ( $F_{2, 116} = 4.246, p < 0.05$ ). In contrast, *post hoc* Bonferroni comparisons within the control groups showed that filopodia-like thin spine density was significantly increased with Rdx-WT (p < 0.001) and Rdx-T564D (p < 0.05), compared to GFP. These effects were not observed in the paired group with GFP and Rdx-WT, while they were maintained with Rdx-T564D (p < 0.01) (Fig. 4C, right).

# Phosphorylated ERM levels in the NAcc core are differentially regulated under the influence of Rdx-WT or Rdx-T564D following AMPH administration

To test whether the expression of Rdx-WT or Rdx-T564D leads to alter radixin signaling in the NAcc core, phosphorylated and total ERM levels were examined by Western blot. The NAcc core tissues obtained from rats expressing GFP, Rdx-WT or Rdx-T564D were obtained at 60 min after





a single IP injection of saline or AMPH (1 mg/kg). Two-way ANOVA conducted on these data revealed a significant effect ( $F_{2, 31} = 8.628$ , p < 0.01) of phosphorylated ERM in the virus condition. Consistent with our previous findings (Kim et al. 2013), we observed a decrease in p-ERM levels in the GFP group following AMPH administration (Fig. 87 A). Notably, a similar trend of decrease in p-ERM levels following AMPH administration was observed in the Rdx-WT group, whereas this effect was not observed and rather high phosphorylated ERM levels were maintained in the Rdx-T564D group (Fig. 87 A). Total ERM protein levels were not significantly different between groups (Fig. 87B).

#### **Discussion**

We previously demonstrated that the artificial expression of a phosphomimetic pseudo-active mutant form of radixin, Rdx-T564D, in the NAcc core disrupted context-independent locomotor sensitization to AMPH (Cai et al. 2022). In the present study, we expanded this concept by including Rdx-WT as well as Rdx-T564D, and exploring their effects on an associated form of drug-induced behaviors. Notably, we found that Rdx-T564D and Rdx-WT have selective inhibitory effects on non-associative locomotor sensitization (Fig. 2B) and associative behaviors (conditioned locomotion and context-specific sensitization) (Fig. 3B) induced by AMPH, respectively.

Both non-associative (context-independent) sensitization by the drug itself and associative (context-specific) sensitization and conditioning through the interaction of the drug and environment contribute to drug addiction development (Anagnostaras et al. 2002; Childs and de Wit 2013; O'Brien et al. 1992; Stewart and Vezina 1988). Although they share similar synaptic transmission mechanisms in the NAcc (Guillory et al. 2022; Kim et al. 2005; Weiss et al. 2000), these processes are regulated by distinct molecular pathways (Singer et al. 2014). For example, pharmacological inhibition of cyclin-dependent kinase 5 activity in the NAcc during systemic AMPH exposure blocked the development of conditioning (Singer et al. 2014), while it enhanced the expression of cocaine-induced locomotor sensitization (Taylor et al. 2007). Similarly, disruption of kalirin-7 function decreased conditioned place preference for cocaine, while it enhanced the expression of locomotor sensitization in kalirin-7 knockout mice (Kiraly et al. 2010). These results suggest that drug-associative conditioning and nonassociative sensitization are modulated by different molecular mechanisms within the NAcc, depending on the actions of specific signaling factors in this region.

In the present study, we used two different types of radixin viral constructs, Rdx-WT and Rdx-T564D. As a

pseudo-active mutant, Rdx-T564D behaves like a constitutively active ERM, whereas Rdx-WT dynamically transitions between its phosphorylated and dephosphorylated states in response to a signaling that the cell receives. Notably, the expression of Rdx-WT and Rdx-T564D in our present study showed divergence in their molecular responses following acute AMPH. The levels of p-ERM in the Rdx-WT group were reduced similarly to those in the GFP group, whereas they were maintained high levels in the Rdx-T564D group (Fig. S7 A). These findings suggest that Rdx-WT and Rdx-T564D produce measurable differences in radixin signaling in the NAcc as evidenced by distinct p-ERM patterns under saline and AMPH conditions. In line with these findings, our results suggest that radixin, depending on its phosphorylation state, may differentially regulate both associative and non-associative drug-induced behaviors.

There is substantial evidence that the structural plasticity of dendritic spines, particularly in the NAcc of brain reward circuitry, is implicated in the development of drug addiction (Nestler 2001; Robinson and Kolb 2004). Consistent with previous findings (Benneyworth and Coyle 2012), we observed that AMPH increased total spine density in rats expressing GFP in the paired group (Fig. 4B). Further analysis of spine subtypes revealed that thin spines primarily contributed to the increase in total spine density (Fig. 4B), while stubby and mushroom spines had no effect (Fig. S6). Notably, when we further categorized thin spines into mature and immature (filopodia-like) subtypes, we found that only the densities of mature thin spines were significantly increased in the paired group, compared to the control group, with GFP (Fig. 4C). Although these effects were maintained with Rdx-T564D, they disappeared with Rdx-WT (Fig. 4B, C). It should be noted that our classification of 'immature' and 'mature' spines is based on morphological criteria such as spine length and head-diameter, and this arbitrary differentiation between immature and mature spines without electron microscopy remains an approximation. To compensate for this limitation, we validated the classification using an immunohistochemical approach that labels AMPA receptor subunits, specifically GluA1. Mature spines contain AMPA receptors and exhibit functional responses to locally uncaged glutamate, making them likely to form functional synapses (Khibnik et al. 2016; Vardalaki et al. 2022). We found that co-labeling of GFP and GluA1 was observed in the morphologically mature spines, but not in the long thinner spines that we characterized as immature (Fig S4). These findings suggest that our morphological classification is consistent with functional markers of maturity of thin spines. Thus, the increase in mature thin spines in the paired group with GFP may reflect the formation of new synapses associating AMPH with its paired environment,



while Rdx-WT may selectively disrupt this process. These results align with the behavioral findings where AMPHinduced conditioned locomotion and context-specific sensitization were selectively disrupted by Rdx-WT, but not by Rdx-T564D (Fig. 3B, C), indicating that associative drug-induced behaviors are regulated by structural plasticity induced by Rdx-WT. Although these effects became slightly less evident when we re-analyzed the same data on a per-animal basis (Fig. S8), additional correlation analysis between conditioned locomotor activity and dendritic spine counts revealed that there was a significant positive correlation between total spine counts and conditioned locomotor activity in Paired group with Rdx-WT (Fig. S9). It was also found that this effect was nearly significant (P = 0.0544) for mature thin spines (Fig. S9), implying that dendritic spines, especially mature thin spines, become more relevant to behavioral output to contextual stimuli in the condition of Rdx-WT overexpression.

Notably, both Rdx-WT and Rdx-T564D increased filopodia-like thin spine densities under basal conditions without drug exposure (Fig. 1B) and in control groups without drug-environment associations (Fig. 4C, right). However, they exhibited differential responses in the AMPH paired group (Fig. 4C, right). Rdx-WT no longer increased filopodia-like thin spines, whereas Rdx-T564D maintained this effect. Dendritic filopodia are structural precursors to new spines and play an essential role in forming new synaptic connections during learning and memory (Portera-Cailliau et al. 2003; Yuste and Bonhoeffer 2004; Ziv and Smith 1996). For instance, activity-dependent filopodia contribute to the formation of new synapses during motor learning (Hedrick et al. 2022), and sleep strengthens these synaptic connections by promoting the filopodia formation and their development into mature spines (Adler et al. 2021). Given this background, the reduction of filopodia-like thin spines in the paired group with Rdx-WT (Fig. 4C, right) suggests a diminished capacity for new synapse formation in this group, whereas the maintained increase in the paired group with Rdx-T564D likely contributes to the preservation of drug-related associative memory formation. The inhibitory effect of Rdx-WT on drug-associated synaptic connections may provide a potentially useful protective mechanism against relapse by reducing the formation of drug-associated memories.

Collectively, our results suggest that Rdx-WT, through which the phosphorylation levels of radixin can be flexibly modulated, plays a greater role in the dynamics of spine structure under conditions of drug and environment associations, whereas Rdx-T564D, with its fixed phosphorylation state as a mutant, is more narrowly effective on non-associative drug effects. The exact molecular mechanisms mediating radixin-induced structural plasticity have

not yet been explored and remain to be investigated. Furthermore, given our limited understanding of the precise functional roles of dendritic spines, it may seem bold to directly associate plastic changes in spines with different types of drug-induced behaviors. Nonetheless, it is clear that dendritic spines play a key role in mediating long-term behavioral changes (Robinson and Kolb 2004; Xu et al. 2009; Yang et al. 2009), and dynamic alterations in spine structure contribute to a complex, multi-stage process in the development of drug addiction (Christian et al. 2017). Considering that AMPH-induced sensitization or conditioning is a form of long-term memory (Anagnostaras et al. 2002; Robinson and Berridge 1993), our findings · that manipulation of radixin (both wildtype and mutant) in the NAcc core can selectively disrupt AMPH-induced behaviors by affecting thin spine plasticity at this site · provide new evidence that ERM proteins are critically involved in mediating addictive behaviors.

In conclusion, our findings revealed that radixin, depending on its flexible or constitutive phosphorylation state, plays a crucial role in regulating the structural plasticity of dendritic spines in the NAcc and related drug-induced behaviors. Specifically, Rdx-WT appears to inhibit the formation of drug-associated synaptic connections, potentially providing a protective mechanism against relapse by reducing the capacity for associative learning in response to drug-environment pairings (see supplementary table for summary of results). These results underscore the importance of radixin in modulating the distinct neuronal processes underlying both associative and non-associative drug-induced behavioral changes.

Supplementary Information The online version contains supplementary material available at https://doi.org/10.1007/s00213-025-06823-w.

Author contributions WTC, WYK and JHK designed the whole experiments. WTC and HR performed the behavioral experiments. WTC, MJK and JH performed the imaging experiments and analyzed imaging data. WTC performed dendritic spine analyses. WTC, WYK and JHK analyzed the whole data. LR and HM designed and provided plasmids for viral vectors. WTC, WYK and JHK wrote the paper. All authors read and approved the final manuscript.

**Funding** This work was supported by the National Research Foundation of Korea funded by the Ministry of Science and ICT (2018R1 A4 A1025230, 2019R1 A2 C1011262, 2022R1 A4 A5033852).

**Data availability** Data will be available from corresponding authors upon reasonable request.

#### **Declarations**

**Competing interests** The authors declare that they have no competing interests.



#### References

- Adler A, Lai CSW, Yang G, Geron E, Bai Y, Gan W-B (2021) Sleep promotes the formation of dendritic filopodia and spines near learning-inactive existing spines. Proc Natl Acad Sci 118(50):e2114856118
- Anagnostaras SG, Schallert T, Robinson TE (2002) Memory processes governing amphetamine-induced psychomotor sensitization. Neuropsychopharmacology 26(6):703–715
- Benneyworth MA, Coyle JT (2012) Altered acquisition and extinction of amphetamine-paired context conditioning in genetic mouse models of altered NMDA receptor function. Neuropsychopharmacology 37(11):2496–2504
- Boileau I, Dagher A, Leyton M, Gunn RN, Baker GB, Diksic M et al (2006) Modeling sensitization to stimulants in humans: an [11 C] Raclopride/positron emission tomography study in healthy men. Arch Gen Psychiatry 63(12):1386–1395
- Bosanquet DC, Ye L, Harding KG, Jiang WG (2014) FERM family proteins and their importance in cellular movements and wound healing. Int J Mol Med 34(1):3–12
- Cahill M, Walker D, Gancarz A, Wang Z, Lardner C, Bagot R et al (2018) The dendritic spine morphogenic effects of repeated cocaine use occur through the regulation of serum response factor signaling. Mol Psychiatry 23(6):1474–1486
- Cai WT, Kim WY, Kwak MJ, Rim H, Lee SE, Riecken LB et al (2022) Disruption of amphetamine sensitization by alteration of dendritic thin spines in the nucleus accumbens core. J Neurochem 161(3):266–280
- Cheron J, Kerchove d'Exaerde A.d (2021) Drug addiction: from bench to bedside. Transl Psychiatry 11(1):424
- Childress AR, McLellan AT, O'Brien CP (1986) Abstinent opiate abusers exhibit conditioned craving, conditioned withdrawal and reductions in both through extinction. Br J Addict 81(5):655–660
- Childs E, de Wit H (2013) Contextual conditioning enhances the psychostimulant and incentive properties of d-amphetamine in humans. Addict Biol 18(6):985–992
- Christian DT, Wang X, Chen EL, Sehgal LK, Ghassemlou MN, Miao JJ et al (2017) Dynamic alterations of rat nucleus accumbens dendritic spines over 2 months of abstinence from extended-access cocaine self-administration. Neuropsychopharmacology 42(3):748–756
- Floresco SB (2015) The nucleus accumbens: an interface between cognition, emotion, and action. Annu Rev Psychol 66(1):25–52
- Freymuth PS, Fitzsimons HL (2017) The ERM protein Moesin is essential for neuronal morphogenesis and long-term memory in Drosophila. Mol Brain 10(1):41
- Furutani Y, Kawasaki M, Matsuno H, Mitsui S, Mori K, Yoshihara Y (2012) Vitronectin induces phosphorylation of Ezrin/radixin/moesin actin-binding proteins through binding to its novel neuronal receptor telencephalin. J Biol Chem 287(46):39041–39049
- Geinisman Y, Berry RW, Disterhoft JF, Power JM, Van der Zee EA (2001) Associative learning elicits the formation of multiple-synapse boutons. J Neurosci 21(15):5568–5573
- Guillory AM, Herrera SH, Baker LK, Bubula N, Forneris J, You Z-B et al (2022) Conditioned Inhibition of amphetamine sensitization. Neurobiol Learn Mem 192:107636
- Hausrat TJ, Muhia M, Gerrow K, Thomas P, Hirdes W, Tsukita S et al (2015) Radixin regulates synaptic GABAA receptor density and is essential for reversal learning and short-term memory. Nat Commun 6(1):6872
- Hedrick NG, Lu Z, Bushong E, Singhi S, Nguyen P, Magaña Y et al (2022) Learning binds new inputs into functional synaptic clusters via spinogenesis. Nat Neurosci 25(6):726–737

- Hyman SE, Malenka RC, Nestler EJ (2006) Neural mechanisms of addiction: the role of reward-related learning and memory. Annu Rev Neurosci 29(1):565–598
- Jaffe JH, Cascella NG, Kumor KM, Sherer MA (1989) Cocaine-induced cocaine craving. Psychopharmacology 97(1):59–64
- Jang JK, Kim WY, Cho BR, Lee JW, Kim JH (2018) Locomotor sensitization is expressed by Ghrelin and D1 dopamine receptor agonist in the nucleus accumbens core in amphetamine pre-exposed rat. Addict Biol 23(3):849–856
- Jung Y, Mulholland PJ, Wiseman SL, Judson Chandler L, Picciotto MR (2013) Constitutive knockout of the membrane cytoskeleton protein beta adducin decreases mushroom spine density in the nucleus accumbens but does not prevent spine remodeling in response to cocaine. Eur J Neurosci 37(1):1–9
- Kawaguchi K, Yoshida S, Hatano R, Asano S (2017) Pathophysiological roles of Ezrin/radixin/moesin proteins. Biol Pharm Bull 40(4):381–390
- Khibnik LA, Beaumont M, Doyle M, Heshmati M, Slesinger PA, Nestler EJ et al (2016) Stress and cocaine trigger divergent and cell type–specific regulation of synaptic transmission at single spines in nucleus accumbens. Biol Psychiatry 79(11):898–905
- Kim J-H, Perugini M, Austin JD, Vezina P (2001) Previous exposure to amphetamine enhances the subsequent locomotor response to a D1 dopamine receptor agonist when glutamate reuptake is inhibited. J Neurosci 21(5):RC133
- Kim JH, Austin JD, Tanabe L, Creekmore E, Vezina P (2005) Activation of group II mGlu receptors blocks the enhanced drug taking induced by previous exposure to amphetamine. Eur J Neurosci 21(1):295–300
- Kim WY, Shin S, Kim S, Jeon S, Kim J-H (2009) Cocaine regulates ezrin–radixin–moesin proteins and RhoA signaling in the nucleus accumbens. Neuroscience 163(2):501–505
- Kim WY, Jang JK, Shin J-K, Kim J-H (2013) Amphetamine dephosphorylates ERM proteins in the nucleus accumbens core and lithium attenuates its effects. Neurosci Lett 552:103–107
- Kiraly DD, Ma X-M, Mazzone CM, Xin X, Mains RE, Eipper BA (2010) Behavioral and morphological responses to cocaine require kalirin7. Biol Psychiatry 68(3):249–255
- Kruyer A, Scofield MD, Wood D, Reissner KJ, Kalivas PW (2019) Heroin cue–evoked astrocytic structural plasticity at nucleus accumbens synapses inhibits heroin seeking. Biol Psychiatry 86(11):811–819
- Lamprecht R, LeDoux J (2004) Structural plasticity and memory. Nat Rev Neurosci 5(1):45–54
- Lanciego JL, Luquin N, Obeso JA (2012) Functional neuroanatomy of the basal ganglia. Cold Spring Harb Perspect Med 2(12):a009621
- Leuner B, Falduto J, Shors TJ (2003) Associative memory formation increases the observation of dendritic spines in the hippocampus. J Neurosci 23(2):659–665
- Nestler EJ (2001) Molecular basis of long-term plasticity underlying addiction. Nat Rev Neurosci 2(2):119–128
- Niggli V, Rossy J (2008) Ezrin/radixin/moesin: versatile controllers of signaling molecules and of the cortical cytoskeleton. Int J Biochem Cell Biol 40(3):344–349
- O'Brien CP, Childress AR, McLELLAN AT, Ehrman R (1992) Classical conditioning in drug-dependent humans. Ann N Y Acad Sci 654:400–415
- Portera-Cailliau C, Pan DT, Yuste R (2003) Activity-regulated dynamic behavior of early dendritic protrusions: evidence for different types of dendritic filopodia. J Neurosci 23(18):7129–7142
- Preston KL, Sullivan JT, Berger P, Bigelow GE (1993) Effects of cocaine alone and in combination with Mazindol in human cocaine abusers. J Pharmacol Exp Ther 267(1):296–307
- Raemaekers T, Peric A, Baatsen P, Sannerud R, Declerck I, Baert V et al (2012) ARF6-mediated endosomal transport of telencephalin



- affects dendritic filopodia-to-spine maturation. EMBO J 31(15):3252–3269
- Riecken LB, Zoch A, Wiehl U, Reichert S, Scholl I, Cui Y et al (2016) CPI-17 drives oncogenic Ras signaling in human melanomas via Ezrin-Radixin-Moesin family proteins. Oncotarget 7(48):78242
- Robinson TE, Berridge KC (1993) The neural basis of drug craving: an incentive-sensitization theory of addiction. Brain Res Rev 18(3):247–291
- Robinson TE, Kolb B (2004) Structural plasticity associated with exposure to drugs of abuse. Neuropharmacology 47:33–46
- Rodriguez A, Ehlenberger DB, Dickstein DL, Hof PR, Wearne SL (2008) Automated three-dimensional detection and shape classification of dendritic spines from fluorescence microscopy images. PLoS ONE 3(4):e1997
- Schubert V, Dotti CG (2007) Transmitting on actin: synaptic control of dendritic architecture. J Cell Sci 120(2):205–212
- Sekino Y, Kojima N, Shirao T (2007) Role of actin cytoskeleton in dendritic spine morphogenesis. Neurochem Int 51(2–4):92–104
- Singer BF, Neugebauer NM, Forneris J, Rodvelt KR, Li D, Bubula N et al (2014) Locomotor conditioning by amphetamine requires cyclin-dependent kinase 5 signaling in the nucleus accumbens. Neuropharmacology 85:243–252
- Stewart J, Vezina P (1988) Conditioning and behavioral sensitization. Sensitization in the nervous system, 207–224
- Taylor JR, Lynch WJ, Sanchez H, Olausson P, Nestler EJ, Bibb JA (2007) Inhibition of Cdk5 in the nucleus accumbens enhances the locomotor-activating and incentive-motivational effects of cocaine. Proc Natl Acad Sci 104(10):4147–4152
- Tiffany ST, Wray JM (2012) The clinical significance of drug craving. Ann N Y Acad Sci 1248(1):1–17

- Vardalaki D, Chung K, Harnett MT (2022) Filopodia are a structural substrate for silent synapses in adult neocortex. Nature 612(7939):323–327
- Vezina P (2004) Sensitization of midbrain dopamine neuron reactivity and the self-administration of psychomotor stimulant drugs. Neurosci Biobehavioral Reviews 27(8):827–839
- Weiss F, Maldonado-Vlaar CS, Parsons LH, Kerr TM, Smith DL, Ben-Shahar O (2000) Control of cocaine-seeking behavior by drug-associated stimuli in rats: effects on recovery of extinguished operant-responding and extracellular dopamine levels in amygdala and nucleus accumbens. Proc Natl Acad Sci 97(8):4321–4326
- Xu T, Yu X, Perlik AJ, Tobin WF, Zweig JA, Tennant K et al (2009) Rapid formation and selective stabilization of synapses for enduring motor memories. Nature 462(7275):915–919
- Yang G, Pan F, Gan W-B (2009) Stably maintained dendritic spines are associated with lifelong memories. Nature 462(7275):920–924
- Yuste R, Bonhoeffer T (2004) Genesis of dendritic spines: insights from ultrastructural and imaging studies. Nat Rev Neurosci 5(1):24–34
- Ziv NE, Smith SJ (1996) Evidence for a role of dendritic filopodia in synaptogenesis and spine formation. Neuron 17(1):91–102

**Publisher's note** Springer Nature remains neutral with regard to jurisdictional claims in published maps and institutional affiliations.

Springer Nature or its licensor (e.g. a society or other partner) holds exclusive rights to this article under a publishing agreement with the author(s) or other rightsholder(s); author self-archiving of the accepted manuscript version of this article is solely governed by the terms of such publishing agreement and applicable law.

